

Tunable LED illumination for biological tissue imaging

Łukasz Gryko,* Jakub Lewandowski

Faculty of Electrical Engineering, Białystok University of Technology, Wiejska 45D, 15-351 Białystok, Poland

Received December 15, 2023; accepted December 29, 2023; published December 31, 2023

Abstract—The article presents the results of biological tissue imaging with a tunable broadband LED illuminator with adjustable color and correlated color temperature of white light characterized by high color rendering indices. Color imaging of tissue is the basis for diagnostic procedures in various disease states. For this reason, it is essential to optimize the illumination so that differences in tissue color are highlighted not only by improved color fidelity but also by high color contrast.

In today's world, technological progress significantly impacts the development of medical fields, enabling ever more precise and effective diagnostic methods. Medical imaging with UV-VIS-NIR light is essential for diagnosing and treating various diseases. Spectral imaging, which includes hyperspectral and multispectral imaging [1] using a multispectral camera [2] or a spectrally tunable source [3], is developing rapidly. One of the innovative tools developed for biological tissue imaging is a tunable broadband LED illuminator (TBLEDI) [4, 5]. This advanced technology makes it possible to obtain high-quality images, which is crucial for accurately diagnosing various diseases and conditions [6–8].

White visible light is commonly used in surgical procedures and routine diagnostics, but the inherent contrast is low [3]. It provides an overall view of tissue structure and allows for identifying abnormalities [9].

The spectral power distribution (SPD) of the light emitted by TBLEDI is crucial for achieving high color contrast in tissue imaging [10]. Thanks to the high resolution of the images and the ability to adapt the SPD of the light to the specificity of the examined tissue, even subtle abnormalities can be detected [8,11,12]. Green [13], red, and near-infrared [14] lights are used in vascular imaging, as well as red light for pigmentation [15], which can help to extract details from tissue.

However, it is still unclear how illumination should be optimized to highlight differences in tissue color and make the selected structures recognizable [16]. Recent reports address the selection of a correlated color temperature (CCT) [9] of the light source or the use of a specific SPD of the light to effectively distinguish the tissue features due to their different spectral properties of absorption and reflection [10,16]. In some cases, especially in cell diagnostics, light filtering has been used to visualize specific structures [17]. However, using single-color LEDs is a much more energy-efficient solution.

Another factor that influences image contrast is the brightness of the emitted light [8]. Therefore, the ability to adjust the illumination intensity is necessary.

Our research aimed to verify the functionality of the developed LED-based [18] imaging system, which enables the observation of essential parameters of the tissue area being diagnosed or treated.

The light from each LED was coupled into the mixing rod via optical PMMA fibers with a diameter of 3 mm. A PMMA mixing rod with a length of 300 mm and a cross-section of 20×20 mm² was used [19, 20]. It was cut at the end at a 45-degree angle and polished. Two diffusers (DG20-120-MD and DG20-220-MD) were attached to the light exit of the rod to increase the homogenization of the sample illumination in the horizontal plane, Fig. 1.

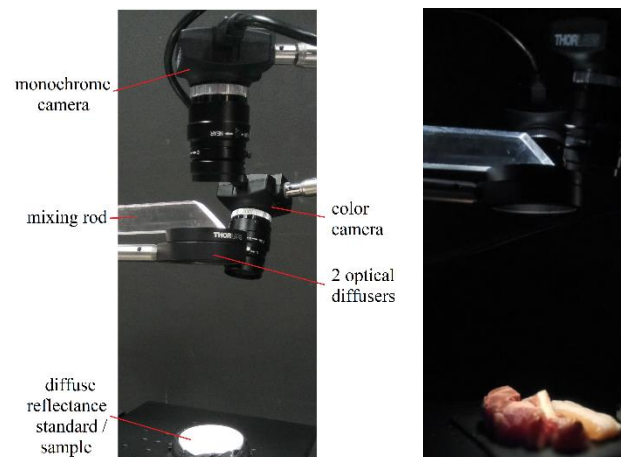


Fig. 1. Laboratory stand during calibration (left) and experiment (right).

The tests included five white light illuminations with CCT in the 2500–6500 K range (Fig. 2) with high color quality indices (R_a , R_9 , R_f , R_g) (Table 1) and an illuminance of 57 lx in the sample plane. The measurements of the light spectra were performed with a Spectis 1.0 spectroradiometer. The tests were also conducted with ten single-color LED lights (420, 450, 470, 490, 515, 525, 590, 620, 630, 660, and 680 nm) [21] with the same irradiance of 15.5 $\mu\text{W}/\text{cm}^2$. The lights' irradiance was chosen so that none overexposed the camera's matrices. The uniformity of the surface illumination was 0.7.

* E-mail: l.gryko@pb.edu.pl

Color (DCC1645C-HQ with an IR-cut filter 650 nm) and monochrome (DCC1545M-GL) CMOS cameras with a resolution of 1280×1024 were placed at 150 mm from the porcine tissues (tendon, fat, bone marrow, bone, and muscle) to capture their images simultaneously, see Fig. 1. The cameras were aligned at a slight angle to avoid specular reflections from the sample. The cameras were equipped with lenses with a focal length of 8 mm and an aperture of f/1.4. The same and constant exposure parameters were set.

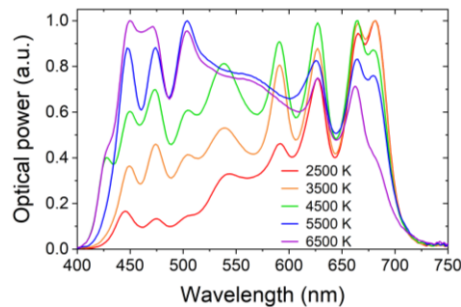


Fig. 2. Spectral power distributions of 2500–6500 K white lights.

Table 1. Parameters of the lights.

CCT (K)	2502	3486	4478	5475	6534
Ra	97	96	99	97	97
R9	95	97	99	94	94
Rf	92	92	95	91	93
Rg	106	99	99	96	97

The color camera images under white lights with high color rendering indices exhibit the actual appearance of the tissues, which allows precise representation of the structure, Fig. 3. Visual analysis of the images indicates that the CCT of the white light should be set for different tissues and adjusted to the spectral reflectance of the sample to correctly detect and distinguish slight differences in its color, which can be associated with disease states.

The color camera images under single color illumination with increased wavelength towards red colors show better color rendition, emphasized shapes, and differentiated darker areas. The best differentiation of tissues is possible at wavelengths from 490 to 590 nm. The qualitative analysis of red tissue (bone marrow) requires illumination in the range above 620 nm. However, analysis at longer wavelengths (> 650 nm) is prevented by an IR-cut filter, which is used as standard in color cameras to ensure correct color rendering.

On the contrary, images taken with a monochromatic camera under single color illumination at shorter wavelengths (420 and 450 nm) show a higher contrast so that details – the boundaries of fibers, fat layers, and muscles- can be better recognized.

Qualitative analysis of pork samples, considering the visible muscle and fat content, can be performed under single-color illumination and provides comparable or even

better results than illumination with white light, as the boundaries between the different tissues are visible.

The local spectral reflectance measurements $R(\lambda)$ (Fig. 4) performed with the Konica Minolta CS2600M reflectometer and the spectral reflectance contrast RC (Fig. 5) provide suggestions for the selection of wavelengths to differentiate tissues:

$$RC = \frac{R_{t1}(\lambda) - R_{t2}(\lambda)}{R_{t1}(\lambda) + R_{t2}(\lambda)} \quad (1)$$

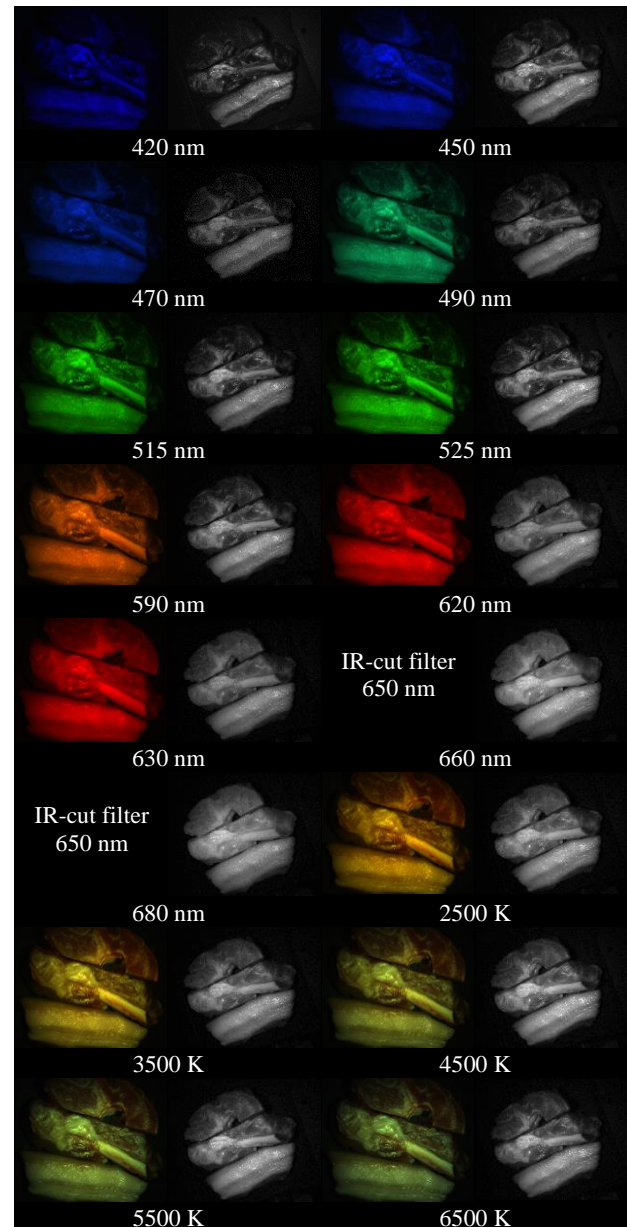


Fig. 3. Images of the samples for single color and white lights with different CCT and high color rendering indices.

The images of the tissues at the single-color illuminations were analyzed by examining the pixel

intensity $I(\lambda)$ (Figs. 5–6), and image contrast C was determined (Fig. 8–9):

$$C = \frac{I_{t1}(\lambda) - I_{t2}(\lambda)}{I_{t1}(\lambda) + I_{t2}(\lambda)} \quad (2)$$

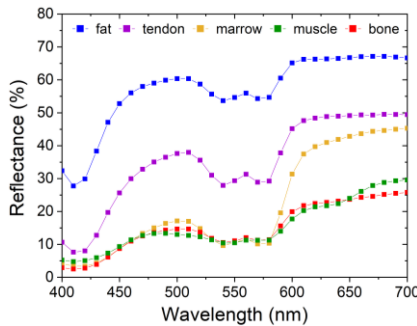


Fig. 4. Spectral reflectance of tissues.

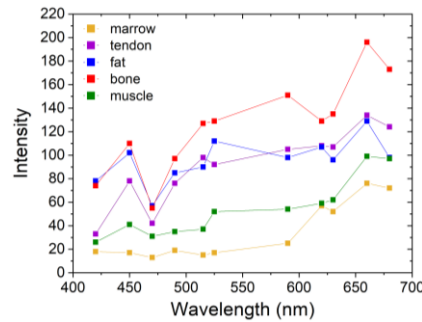


Fig. 5. Pixel intensity values of the tissue images with a monochrome camera under single color lights with different wavelengths.

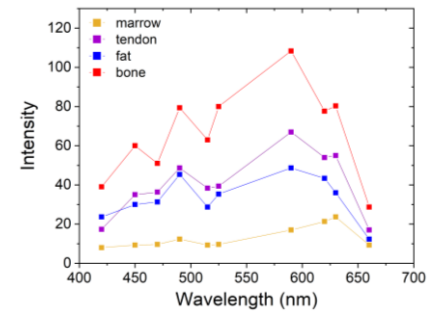


Fig. 6. Average pixel intensity values of the tissue images with a color camera under single color lights with different wavelengths.

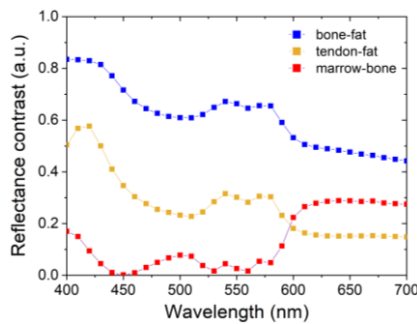


Fig. 7. Spectral reflectance contrast of tissues.

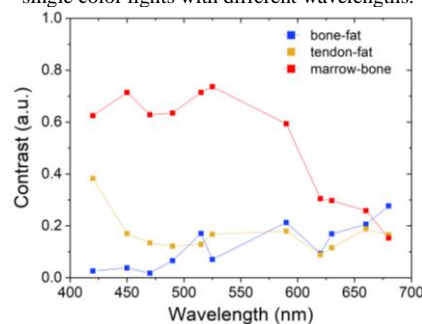


Fig. 8. Spectral contrast of tissues, images taken with a monochrome camera under single color lights with different wavelengths.

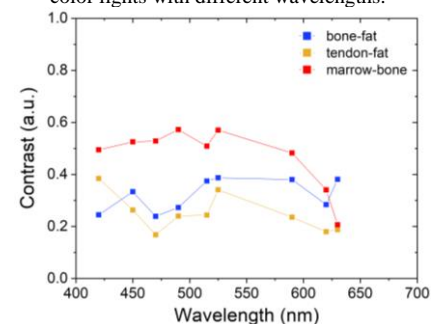


Fig. 9. Spectral contrast of tissues, images taken with a color camera under single color lights with different wavelengths.

Select the wavelength where the reflectance contrast between tissues is highest to increase the contrast between different tissues (Fig. 7). The image contrast of tissues only partially confirms this relationship. To distinguish tendon from fat should be used wavelength 420 nm, which all measurements confirm. Image contrast suggests wavelengths from 420 nm to 590 nm to distinguish bone and marrow, whereas reflectance contrast suggests wavelengths over 600 nm.

When comparing the measurements of both cameras (Fig. 5 and 6), it becomes clear that the position of the camera matrix in relation to the sample is a crucial aspect due to the variable angular distribution of the reflection of tissues. This will be the subject of further specialized tests.

In summary, TBLEDI is an innovative diagnostic tool that revolutionizes the approach to tissue imaging and enables the investigation of them in a way that was previously difficult to achieve. Thanks to the flexibility in setting the illumination parameters, TBLEDI can be used for different examinations, making it a versatile diagnostic tool. It allows doctors to see even the most minor details, which is crucial for a quick and accurate diagnosis.

The research project was funded by the National Science Centre based on decision No. 2021/05/X/ST7/01824.

References

- [1] M.H. Tran, B. Fei, *J. Biomed. Opt.* **28**, 4 (2023).
- [2] E.J.M. Baltussen, E.N.D. Kok, S.G.J. Brouwer de Koning, *J. Biomed. Opt.* **24**, 1 (2019), doi:10.1117/1.JBO.24.1.016002.
- [3] N.T. Clancy, G. Jones, L. Maier-Hein, D.S. Elson, D. Stoyanov, *Med. Image Anal.* **63**, 101699 (2020), doi:10.1016/j.media.2020.101699.
- [4] R. Zhang, Z. Guo, Y. Chen, *IEEE Trans. Instrum. Meas.* **72**, 1 (2023).
- [5] P. Liu, H. Wang, Y. Zhang, *Opt. Commun.* **319**, 133 (2014).
- [6] J. Shen, S. Chang, H. Wang, Z. Zheng, *Light. Res. Technol.* **51**(1), 99 (2019).
- [7] K. Kameyama, T. Ohbayashi, K. Uehara, A. Koga, Y. Hata, *Yonago Acta Med.* **63**(4), 266 (2020), doi:10.33160/yam.2020.11.004.
- [8] H. Wang, R.H. Cuijpers, M.R. Luo, I. Heynderickx, Z. Zheng, *J. Biomed. Opt.* **20**(1), 015005 (2015), doi:10.1117/1.JBO.20.1.015005.
- [9] J. Munding and K. Houser, *Light. Res. Technol.* **51**(2), 280 (2019).
- [10] M.A. Ilişanu, F. Moldoveanu, A. Moldoveanu, *Sensor* **23**(8), 3888 (2023).
- [11] K.L. Hanlon, G. Wei, L. Correa-Selm, J.M. Grichnik, *J. Biomed. Opt.* **27**(8), (2022), doi:10.1117/1.JBO.27.8.080902.
- [12] O.V. Mamontov, A.V. Shcherbinin, R.V. Romashko, *App. Scien.* **10**(18), 6192 (2020), doi:10.3390/app10186192.
- [13] F.J. Burgos-Fernández, *Biomed. Opt. Expr.* **13**(6), 3504 (2022).
- [14] D. Kapsokalyvas, N. Brusino, *Opt. Expr.* **21**(4), 4826 (2013).
- [15] J. Yang, H. Xu, F. Zhang, Z. Wang, P. Xu, *Opt. Eng.* **57**(7), 1 (2018).
- [16] N. Posner, A. Stefanidi, J. Hanhart, *Biomed. Eng. Res.* (2020), <http://resolver.tudelft.nl/uuid:93142809-9c57-46fb-8ee4-cb61cf1c7178>
- [17] U.J. Błaszczyk, L. Gryko, A. Zajac, *Proc. SPIE* **10445**, 104453Y (2017), doi:10.1117/12.2281095.
- [18] L. Gryko, U.J. Błaszczyk, A.S. Zajac, *Proc. SPIE* **10808**, 1080811 (2018), doi:10.1117/12.2501631.
- [19] U.J. Błaszczyk, L. Gryko, A.S. Zajac, *Metrol. Meas. Syst.* **26**(1), 153 (2019), doi:10.24425/mms.2019.126332.
- [20] U.J. Błaszczyk, M. Gilewski, L. Gryko, A.S. Zajac, *Przegląd Elektrotechniczny* **92**(9), 150 (2016), doi:10.15199/48.2016.09.39.